AD-A185 395 THE PRODUCTION OF ULTRASMALL AND SUPERFINE HOLOGRAPHIC 1/1
DIFFRACTION GRATIN (U) OREGON UNIV EUGENE INST OF
THEORETICAL SCIENCE P L CSONKA FEB 87 AFOSR-TR-87-0963
UNCLASSIFIED $AFOSR-85-0326 F/G 20/6 NL

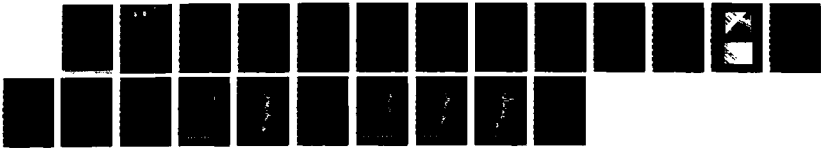

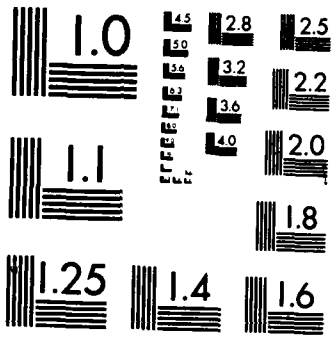

MICROCOPY RESOLUTION TEST CHART
NATIONAL BUREAU OF STANDARDS-1963-A

UNCLASSIFIED
SECURITY CLASSIFICATION OF THIS PAGE

DTIC FILE COPY (2)

AD-A185 395

REPORT DOCUMENTATION PAGE

DTIC ELECTE S OCT 0 1 1987 D

1a. REPORT SECURITY CLASSIFICATION: UNCLASSIFIED	1b. RESTRICTIVE MARKINGS
2a. SECURITY CLASSIFICATION AUTHORITY	3. DISTRIBUTION / AVAILABILITY OF REPORT: Approved for public release; distribution unlimited
2b. DECLASSIFICATION / DOWNGRADING SCHEDULE	
4. PERFORMING ORGANIZATION REPORT NUMBER(S)	5. MONITORING ORGANIZATION REPORT NUMBER(S): AFOSR-TR- 87-0963
6a. NAME OF PERFORMING ORGANIZATION: University of Oregon; 6b. OFFICE SYMBOL (If applicable):	7a. NAME OF MONITORING ORGANIZATION: AFOSR
6c. ADDRESS (City, State, and ZIP Code): Institute of Theoretical Science, Eugene, Oregon	7b. ADDRESS (City, State, and ZIP Code): Building 410, Bolling AFB DC 20332-6448
8a. NAME OF FUNDING / SPONSORING ORGANIZATION: same as 7a; 8b. OFFICE SYMBOL (If applicable): NP	9. PROCUREMENT INSTRUMENT IDENTIFICATION NUMBER: AFOSR 85-0326
8c. ADDRESS (City, State, and ZIP Code): same as 7b	10. SOURCE OF FUNDING NUMBERS: PROGRAM ELEMENT NO. 61102F; PROJECT NO. 2301; TASK NO. A1; WORK UNIT ACCESSION NO.

11. TITLE (Include Security Classification) "THE PRODUCTION OF ULTRASMALL & SUPERFINE HOLOGRAPHIC DIFFRACTION GRATINGS USING SYNCHROTRON RADIATION AND LITHOGRAPHIC TECHNIQUES" (U)

12. PERSONAL AUTHOR(S): Dr Paul L. Csonka

13a. TYPE OF REPORT	13b. TIME COVERED	14. DATE OF REPORT (Year, Month, Day)	15. PAGE COUNT
Annual/Final	FROM 1 Sep 85 TO 31 Dec 86	Feb 87	19

16. SUPPLEMENTARY NOTATION

17. COSATI CODES			18. SUBJECT TERMS (Continue on reverse if necessary and identify by block number)
FIELD	GROUP	SUB-GROUP	Radiation, Lithographic

19. ABSTRACT (Continue on reverse if necessary and identify by block number)

The research effort was directed toward the production of superfine X-ray gratings by holographic means, i.e. generating an interference pattern by X-rays emitted in the form of synchrotron radiation from a high energy electron storage ring, recording the pattern on a resist, such as PMMA, and subsequently transferring it onto metal.

20. DISTRIBUTION / AVAILABILITY OF ABSTRACT: ☒ UNCLASSIFIED/UNLIMITED ☐ SAME AS RPT ☐ DTIC USERS	21. ABSTRACT SECURITY CLASSIFICATION: Unclassified
22a. NAME OF RESPONSIBLE INDIVIDUAL: Dr Howard R. Schlossberg	22b. TELEPHONE (Include Area Code): 202/767-4906; 22c. OFFICE SYMBOL: NP

DD FORM 1473, 84 MAR — 83 APR edition may be used until exhausted. All other editions are obsolete.

SECURITY CLASSIFICATION OF THIS PAGE
UNCLASSIFIED

ANNUAL/FINAL TECHNICAL REPORT

AFOSR-TR- 87-0963

Report of Activity

On Grant Number: AFOSR-85-0326

Title: "The Production of Ultrasmall and Superfine Holographic Diffraction Gratings Using Synchrotron Radiation and Lithographic Techniques"

Period Covered: September 1, 1985 to ~~June 30~~ DEC 31 per HRS, 1986

Report prepared by: Paul L. Csonka
Institute of Theoretical Science
University of Oregon
Eugene, Oregon 97403

Accesion For
NTIS CRA&I
DTIC TAB
Unannounced
Justification
By
Distribution/
Availability Codes
Dist | Avail and/or Special
A-1

DTIC COPY INSPECTED

During the first ten months of this project we have accomplished the goals for the corresponding period as set forth in the original proposal, and in one area (research on multilayered mirrors) we went beyond what we had proposed to accomplish.

Our research effort has been directed toward the production of superfine X-ray gratings by holographic means, *i.e.*, generating an interference pattern by X-rays emitted in the form of synchrotron radiation from a high energy electron storage ring, recording the pattern on a resist, such as PMMA, and subsequently transferring it onto metal.

The work accomplished to date can be divided into three main areas.

(1) Testing the sensitivity and resolution of various resist materials as a function of X-ray energy (betweeen 100 and 1000 eV) and dosage. This study will be needed during the next phase of our project, when the most appropriate energy, dosage and resist material will have to be selected for various grating line densities.

(*a*) Testing of Resist Sensitivity

We prepared a collection of PMMA samples, and sequentially exposed them to X-ray radiation of various energies and dosage. The X-ray energy was varied between 100 eV and 1000 eV. The dosage was increased from about one order of magnitude below what we expected near optimal dosage, to about one order of magnitude above it, typically in a geometrical series of up to ten dosage steps.

All PMMA samples were prepared under identical, well-controlled conditions.

X-ray radiation emerged from Beamline V of the SPEAR storage ring at Stanford. The radiation was generated by the 10 pole and 24 pole wigglers in that beamline. The wiggler magnet gap was varied between 10.5 and 14 cm for the former wiggler, and from 4.5 cm upward for the latter one. By varying the gap size, the wiggler parameter, K, was adjusted, and in this manner the energy of the radiated photons was selected. Either the first or the third radiated harmonic was used. In the latter case the first harmonic was eliminated by filtering the radiation.

We were able to reach the lower photon energies of the indicated range by avoiding the use of any window located between the exposed resist and the high vacuum where the photons were generated. Instead, we employed an externally cooled differential section designed by us. Across this device the vacuum decreased by at least five orders of magnitude (depending on the chemical composition of the gas) without the interposition of any material layer between the photon source and the resist.

The photon intensity could be altered with high accuracy by the use of a "chopper wheel" which had been built by us earlier, for such types of experiments.

Each exposed sample contains up to 12 exposed sites. These have been developed, and are now being analyzed.

Figure 1 shows the boundary of a region exposed to $E_\gamma = (1079 \pm 50)$ eV photons for $T = 20$ sec, as registered on PMMA. The overlaid mask in the corner serves to calibrate. In Figure 2 one can observe strands of PMMA lifted off the surface as a result of intense radiation exposure (E_γ as above, but $T = 60$ sec).

(*b*) Testing of Resist Resolution.

In order to test the resolution of resists down to an interval δ_a, it is necessary to generate radiation patterns which contain features of size δ_a. Since we are interested in δ_a of a few hundred Å, radiation features of such size had to be generated on the resist surface. Since, further, no gratings with line density $\gtrsim 1/\delta_a$ exist at the present time, we produced the needed features by establishing a Fresnel interference pattern from an "optical" grating (*i.e.*, one with line density $\lesssim \frac{1}{2}\,\ell/\mu\text{m}$). These features were imprinted on each resist, for every wavelength and dosage which was studied.

A full analysis of the above requires high resolution microscopy. That is in progress.

In addition to studying the sensitivity and resolution of properties of PMMA, we also investigated the sensitivity and resolution of an amorphous resist made available to us from the Lawrence Berkeley National Laboratory (where it is now in the process of development) as well as two proprietary resists from the Micronix Co. of San Jose, California. Although we do not know the composition of the latter two resists, our agreement with Micronix stipulates that should either or both of their resists prove to be advantageous for our program, they will be made available to us upon request.

For purposes of correctly predicting the generated Fresnel interference pattern, we could not make use of the existing calculations now in general use. The reason is that in the usual approach one neglects the variation in the real part of the index of refraction of the material through which the imprinting radiation passes. We realized, however, that such an approximation is not adequate. Consequently, we developed software which takes into account the variation of both the real, as well as the imaginary part of the index of refraction. [R. Redaelli, R. O. Tatchyn, P. Pianetta, *SPIE Conference on Optical Microlithography,* Santa Clara, March 1986.]

Figure 3 shows a typical calculated Fresnel interference pattern for the intensity of X-ray radiation transmitted through a single slit of diameter 0.5 μm. The photon energy is 1500 eV contained within a 10% total energy bandpass. The slit is assumed to be cut in a layer of gold 0.3 μm thick, located at a distance of 50 μm from the surface on which the Fresnel pattern is evaluated. This figure is to be compared with Figure 4, which displays the prediction for the above case, based on the (unsatisfactory) assumption that the real part of the index of refraction is not changed by the presence of the material. The differences are clearly observable.

Figures 5 and 6 may be similarly contrasted. They show the expected Fresnel interference pattern in the case when the situation is as above, except that the X-ray energy has a full bandpass of 1 keV, centered on 1500 eV, and the slit is located at a distance 100 μm from the surface. In Figure 5 the variation of the real part of the index of refraction is properly taken into account, while in Figure 6 it is neglected. In this case, too, the differences are essential; for example, the central peak of Figure 5 is totally absent in Figure 6.

(2) Instrument Construction.

(*a*) The monochromator will enable us to use X-ray sources which produce broadband radiation. An example is the radiation of Beamline V at SPEAR. We hope to utilize that radiation once again, when the ring starts operating this fall.

The monochromator contains a grating which serves to diffract radiation. It also is designed to include two cylindrical mirrors, and appropriate slits. One of the mirrors focuses the incoming radiation on the receiving slit, the other focuses it through the grating onto the exit slit, from where radiation of the chosen wavelength is projected to the interferometer. The curvature of both mirrors is selected by appropriately setting the mirror benders which hold both mirrors in place. This design offers considerable flexibility, because it will allow us to

vary either or both curvatures. All components of the monochromator are to be located in a vacuum chamber.

So far both mirror benders have been designed and built, both mirrors have been designed and are in the process of being built. The vacuum chamber has not yet been constructed.

(*b*) In the interferometer the incoming (monochromatized) beam is split and two branches are produced. Each branch is incident on a mirror of its own (two mirrors altogether) and the two branches are reunited at the interference regions where the interference pattern is generated and recorded on a resist. This instrument was also designed for maximum flexibility: either one of the mirrors can be removed. The entire interferometer is housed in a vacuum chamber.

All components of the interferometer, as well as its vacuum chamber have been built and are ready for use.

(3) Development of Multilayered Mirrors.

Simultaneously with the activities listed above, we are exploring ways to improve monochromatization and increase throughput by the use of multilayered mirror coatings. It appears that this new technology can be used to advantage in our program, in the 50–100 eV energy range, and possibly at higher energies as well. Simplifying somewhat, one can say that an instrument in which monochromatization is achieved by a grating, is expected to have an energy throughput of $\lesssim 10\%$, while a multilayered mirror coating can in principle achieve a throughput of $\gtrsim 40\%$. On the other hand, while a given grating can select a narrow bandpass over a wide range of energies, any given multilayer is restricted to a relatively narrow energy range, biased in favor of lower energies, and is likely to have a broader bandpass. In certain cases, such as when the photon energy is in the 50–100 eV range and when relatively small superfine gratings are to be produced, monochromatization with the help of multilayers holds out the promise of superior performance. Accordingly, we pursued our research as follows:

(*a*) We prepared two multilayer coated spherical mirrors, designed specifically for use with photons of energy 62.7 eV near normal incidence. (This energy is one of those which are of special interest to this project.)

(*b*) Several multilayers and multilayered echelons were constructed, containing very thin layers (down to a thickness of only two or three atomic radii). At the same time the number of layer pairs was increased to several hundred, in order to improve reflectivity for X-rays with energy near 1 keV at normal incidence.

To our knowledge, no such multilayers have ever been made in the past.

The reflectivity and bandpass of these layers were tested for two types of layered structures. First, layers of tungsten alternating with carbon layers; and second, layers of molybdenum interposed between silicon layers.

Figures 7–10 show typical results. The reflected intensity, proportional to the observed photon counts, is displayed as a function of twice the angle of reflection (θ) in degrees. The lighter curve shows the photon count, while a quantity which is proportional to the logarithm of the photon count is plotted by the darker curve.

Figures 7(a) and 7(b) depict results from a multilayer containing $n = 402$ layers of Si and 402 layers of Mo, when the distance, b, measured from the center of one layer of one kind to the center of the next layer of the same kind, is 23 Å. In addition to the peak near zero degrees, three peaks are clearly distinguishable (at 2θ near 4°, 8° and 12°); their presence demonstrates high quality. Figure 8 shows the first peak (at 2θ near 8°) for a Si–Mo multilayer, when $n = 342$ and $b = 11$ Å. The presence of this peak demonstrates that a multilayer structure exists even at these extremely low b values, when the thickness of any single layer in a pair of layers is close to only two atomic diameters (The present equipment does not allow the deposition of lay-

ers with smaller b. However, we expect the equipment to be modified, and then we will try to reach the lowest possible b values, namely, those where peaks can no longer be distinguished.)

Figures 9(a) and 9(b) refer to C-W multilayers with $n = 120$ and $d = 25$ Å. Four peaks are visible. The first peak from C-W multilayer with $n = 480$ and $d = 9$ Åis shown in Figure 10. (A C-W multilayer with $d = 6$Åshowed no peaks present. That is an indication that at such extremely low b values the multilayered structure can no longer exist. We will confirm that, and also look between $b = 6$ and 9 Å.

(c) We are testing the hypothesis that the reflectivity of multilayers can be improved if the thickness of all layers is near an integer times the average diameter of atoms inside each layer. We expect this phenomenon, because it is known that reflectivity improves when the boundary between layers is sharper. On the other hand, it is reasonable to expect that if a layer is on the average, say, 2.5 atoms thick, instead of either 2 or 3, then the *extra* half-atom will show up as *extra* layers only partially filled, *i.e.*, layers which contain a mixture of both types of atoms. These layers represent a blurring of the boundaries, and thus should decrease reflectivity. Consequently, one expects the following:

If a sequence of multilayer samples is prepared, each sample containing layers of a given thickness, and the thickness of one or both layer types is gradually increased as one goes from one sample to the next, then the reflectivity should go through maxima at those thicknesses which satisfy the above stated *integer condition*. This phenomenon is expected to be more pronounced for thinner layers.

We are in the process of testing this hypothesis. If confirmed, it could yield a simple method to improve the quality and performance of multilayer optics for X-rays.

The research described in Section (3) goes beyond the program originally proposed by us. We believe that these investigations contribute significantly to the understanding of this new technology and, in particular, it will enhance our ability to monochromatize X-ray radiation and to produce high quality interference patterns.

During the first ten months of this project we have thus essentially assembled the equipment and the needed tools to pass to the production phase of holographic X-ray gratings during the second stage or our funded project. However, before actual production can commence, we will have to purchase the equipment budgeted for the next grant year, scheduled to start September 1, 1986. The weakest link in the chain of activities to be performed is the one partly beyond our control, namely, it depends on the availability of wiggler or undulator radiation in the energy range near 100 eV. Such radiation cannot be generated at NBS, nor at Cornell. Of all the storage rings in this country, that leaves only NSLS at Brookhaven, or SPEAR at SSRL. The Synchrotron Radiation Center in Wisconsin may eventually produce such radiation, but only late in the fall, the earliest. At the present, SPEAR is in a period of long shutdown, and will come online only in the fall, several months hence. We are making preparations to insure access to the needed radiation when SPEAR starts operating again.

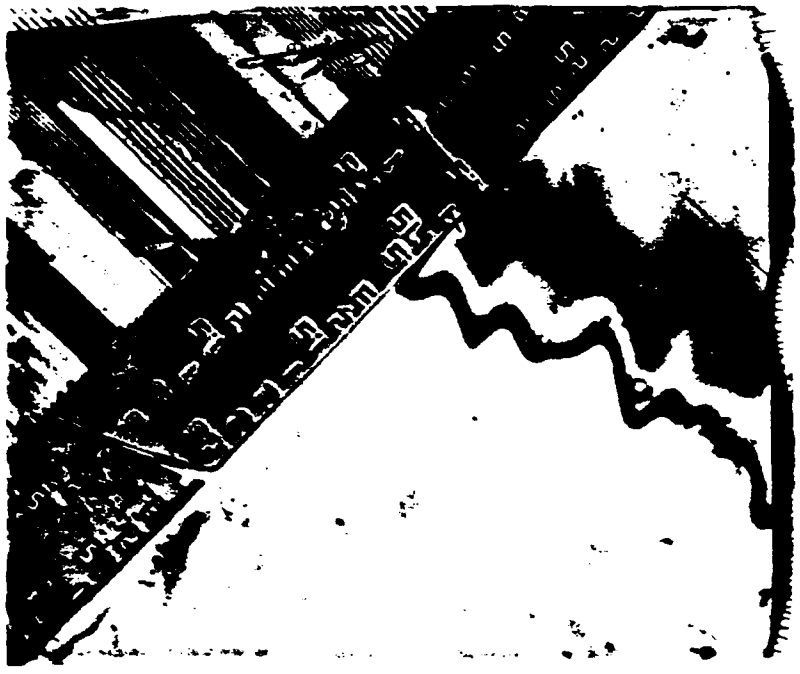

Fig. 1.

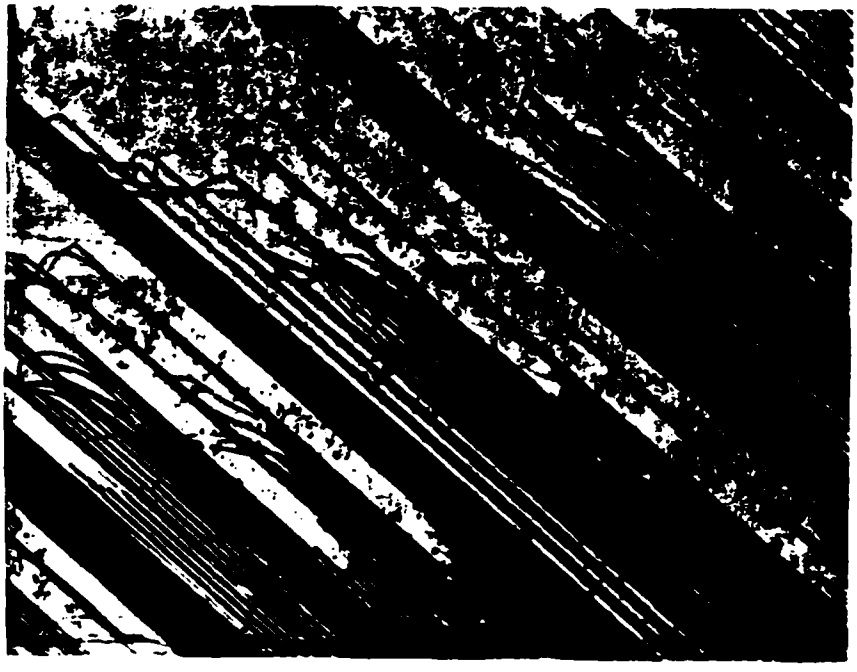

Fig. 2

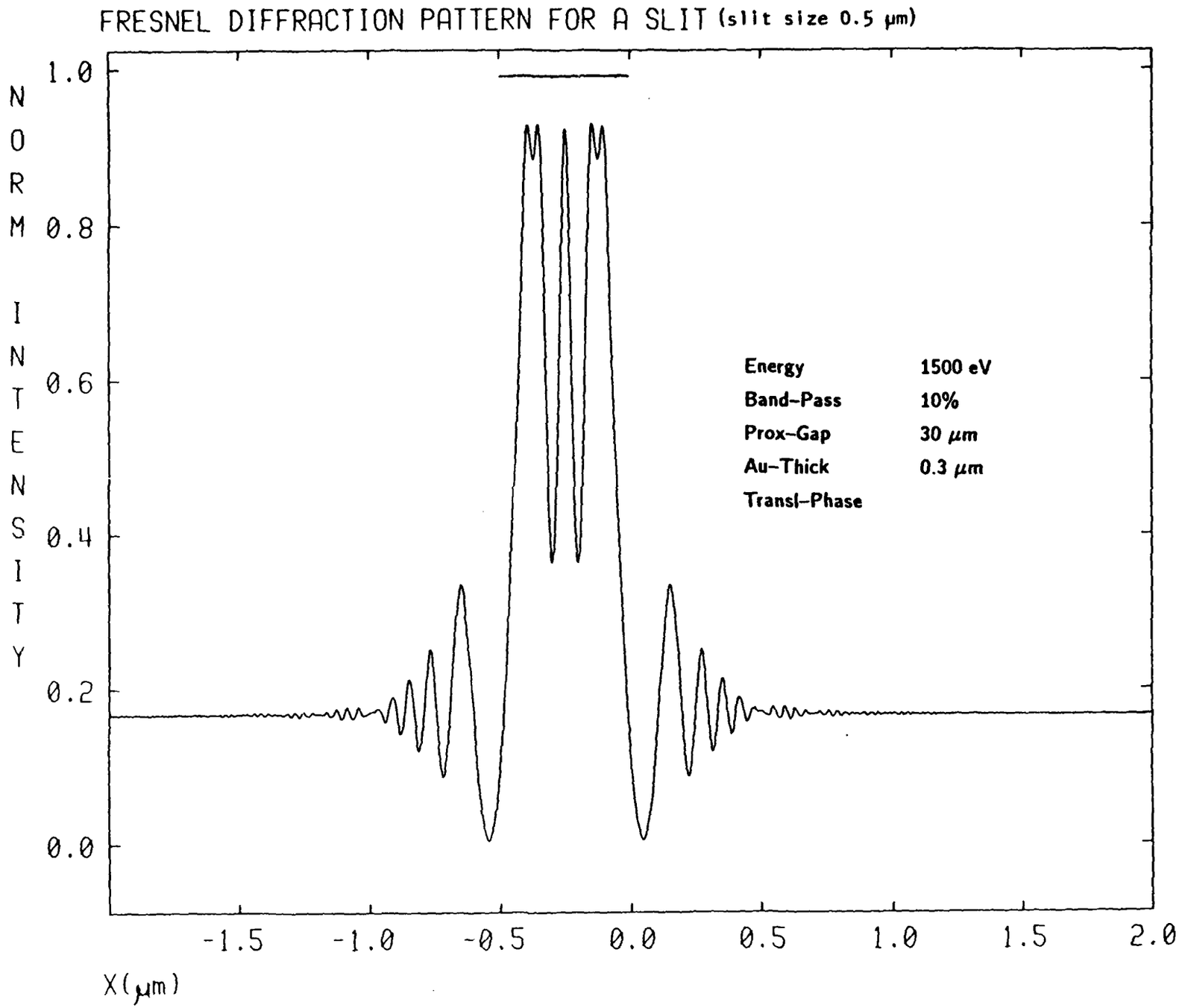
FRESNEL DIFFRACTION PATTERN FOR A SLIT (slit size 0.5 μm)
NORM INTENSITY
1.0
0.8
0.6
0.4
0.2
0.0
-1.5
-1.0
-0.5
0.0
0.5
1.0
1.5
2.0
X(μm)
Energy 1500 eV
Band-Pass 10%
Prox-Gap 30 μm
Au-Thick 0.3 μm
Transl-Phase

Figure 3

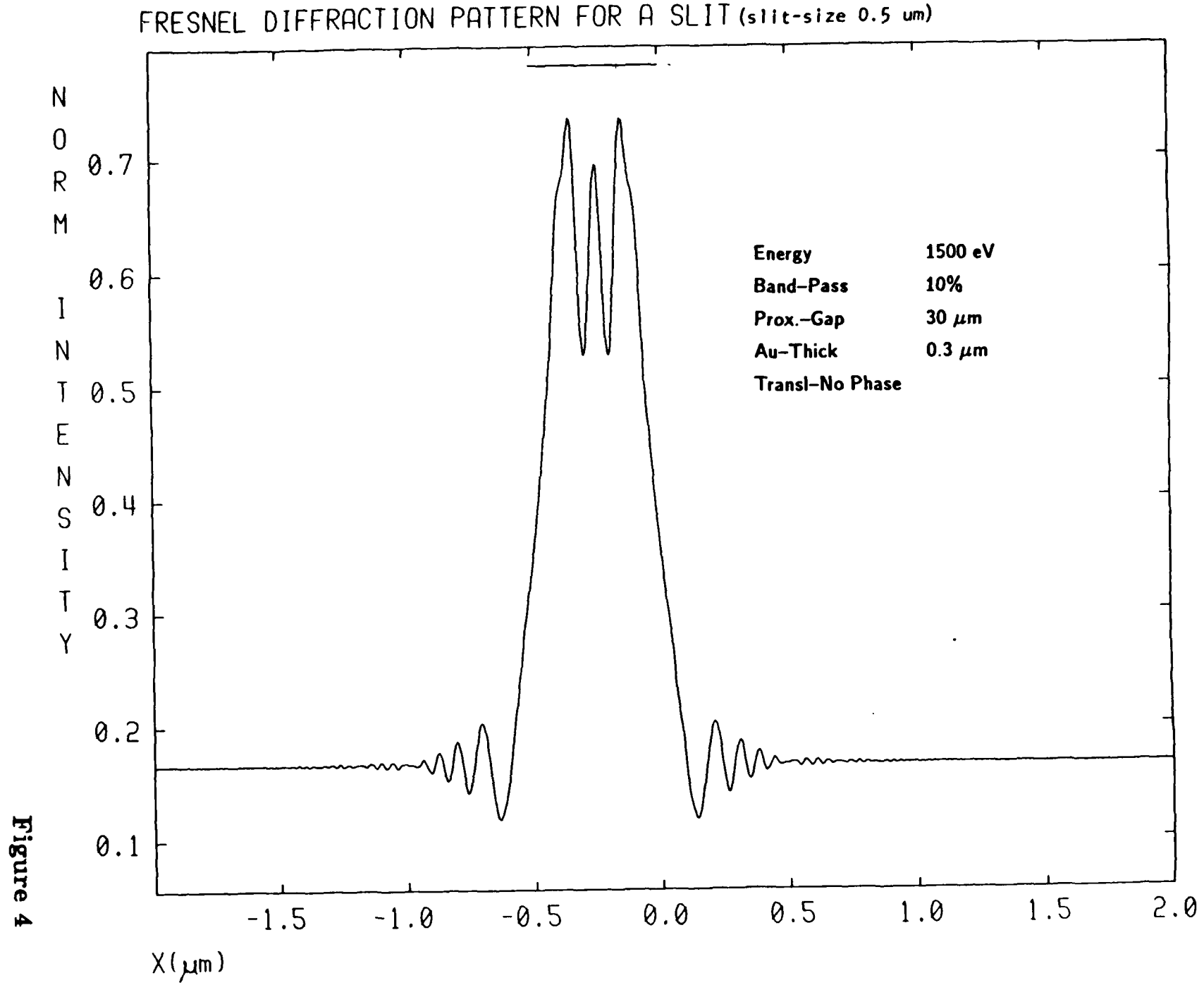
FRESNEL DIFFRACTION PATTERN FOR A SLIT (slit-size 0.5 um)
NORM INTENSITY
0.7
0.6
0.5
0.4
0.3
0.2
0.1
-1.5
-1.0
-0.5
0.0
0.5
1.0
1.5
2.0
X(μm)
Energy 1500 eV
Band-Pass 10%
Prox.-Gap 30 μm
Au-Thick 0.3 μm
Transl-No Phase

Figure 4

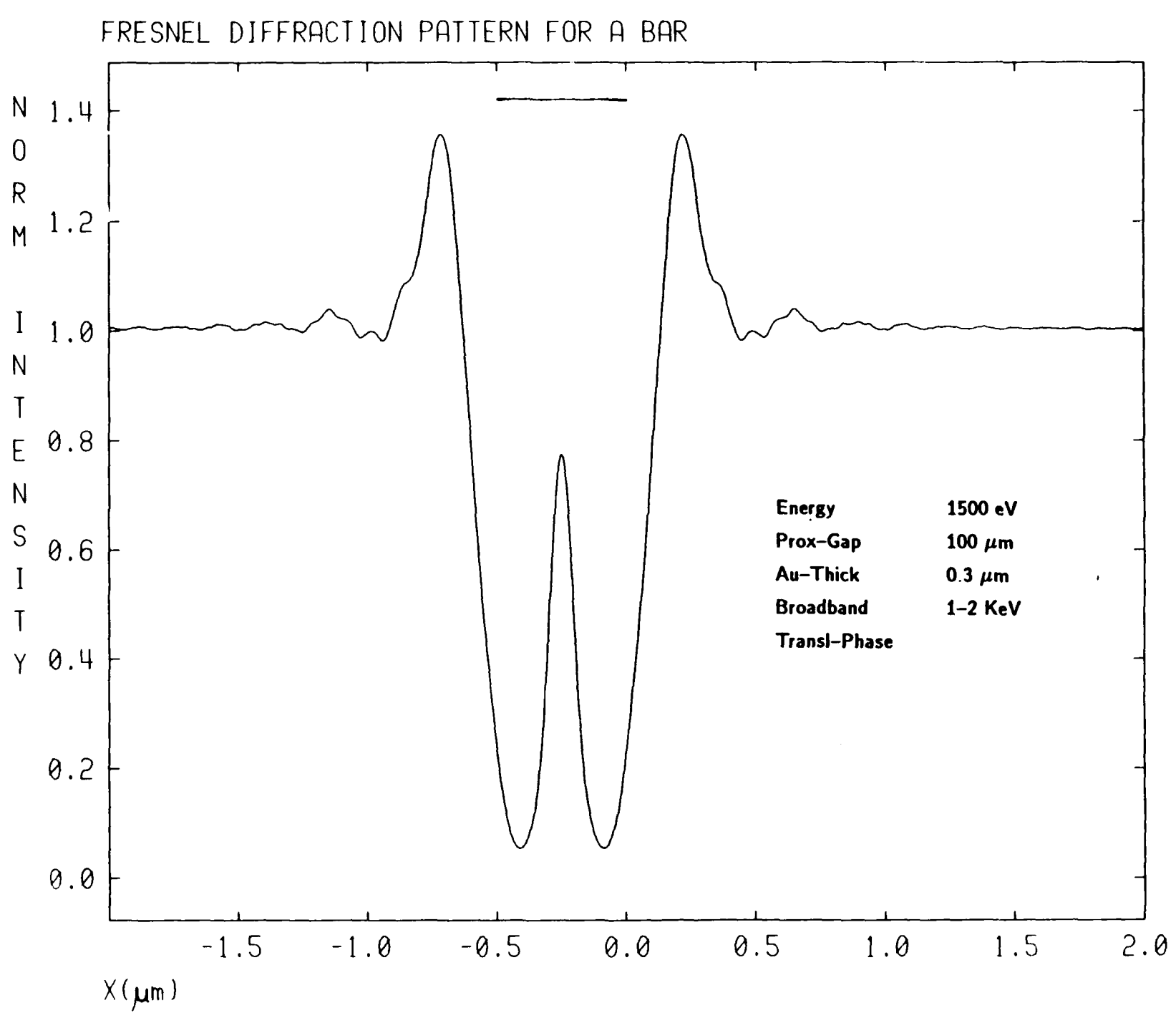
FRESNEL DIFFRACTION PATTERN FOR A BAR
NORM INTENSITY
1.4
1.2
1.0
0.8
0.6
0.4
0.2
0.0
-1.5
-1.0
-0.5
0.0
0.5
1.0
1.5
2.0
X(μm)
Energy 1500 eV
Prox-Gap 100 μm
Au-Thick 0.3 μm
Broadband 1-2 KeV
Transl-Phase

Figure 5

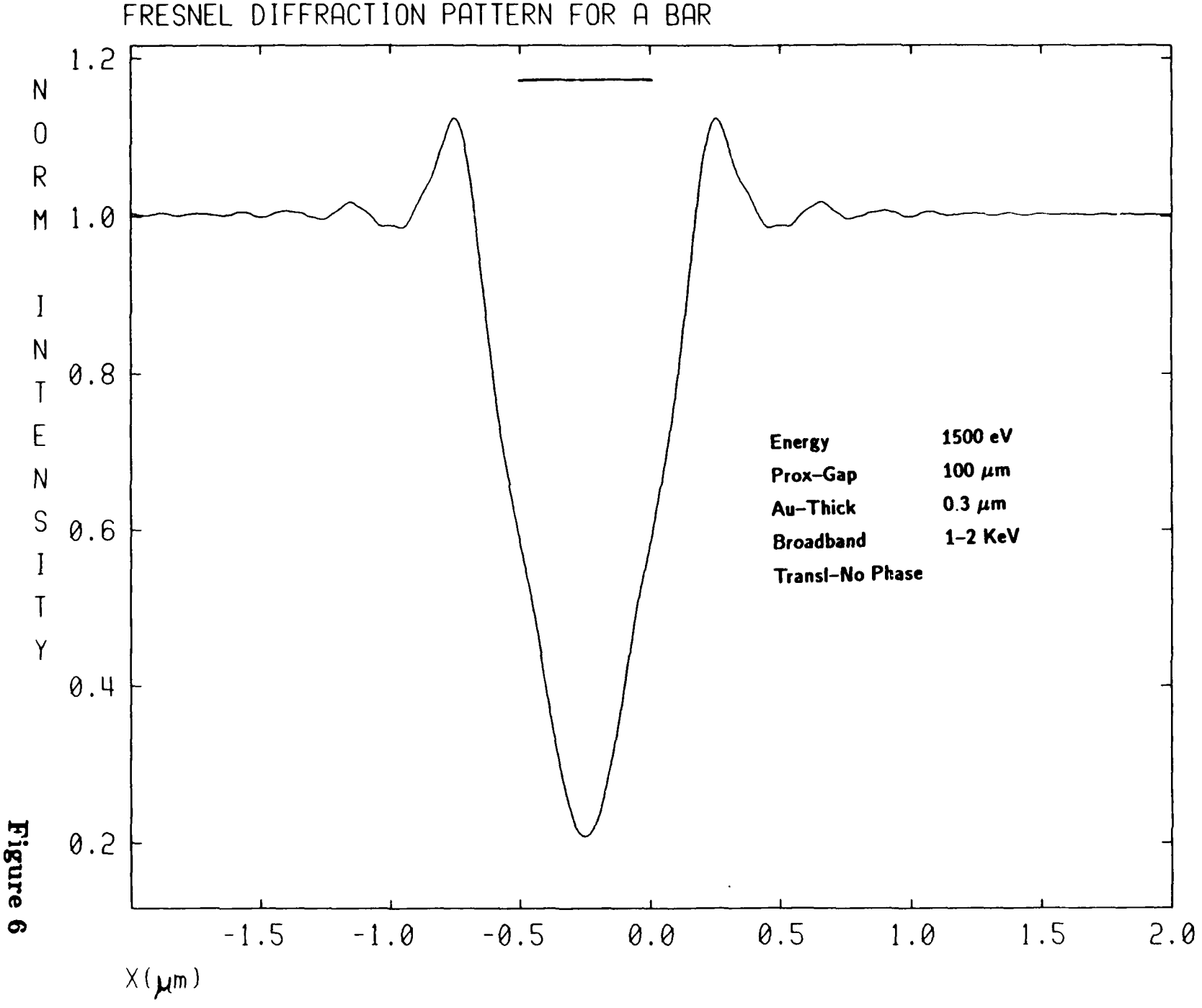
FRESNEL DIFFRACTION PATTERN FOR A BAR
NORM INTENSITY
1.2
1.0
0.8
0.6
0.4
0.2
-1.5
-1.0
-0.5
0.0
0.5
1.0
1.5
2.0
X(μm)
Energy 1500 eV
Prox-Gap 100 μm
Au-Thick 0.3 μm
Broadband 1-2 KeV
Transl-No Phase

Figure 6

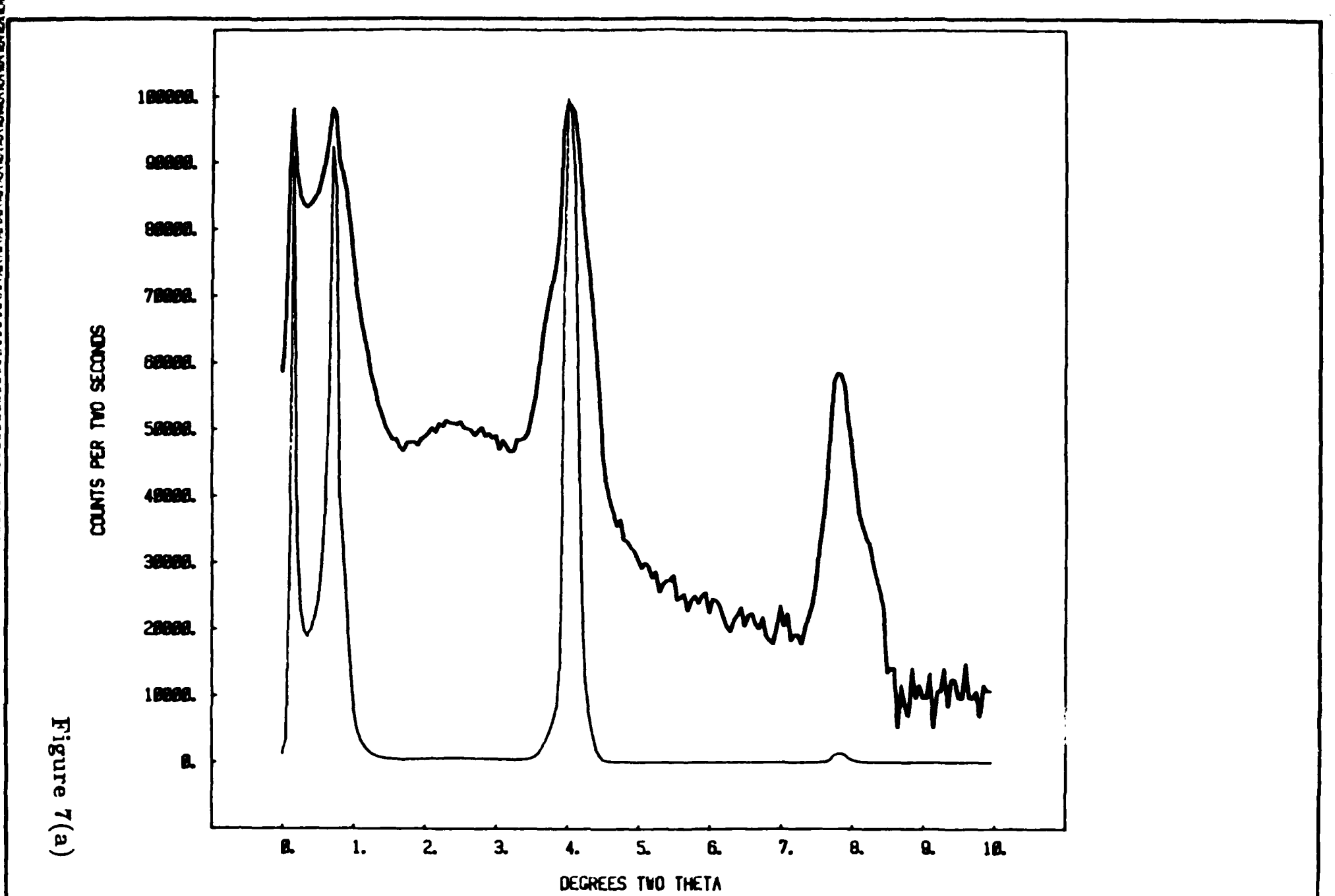

Figure 7(a)

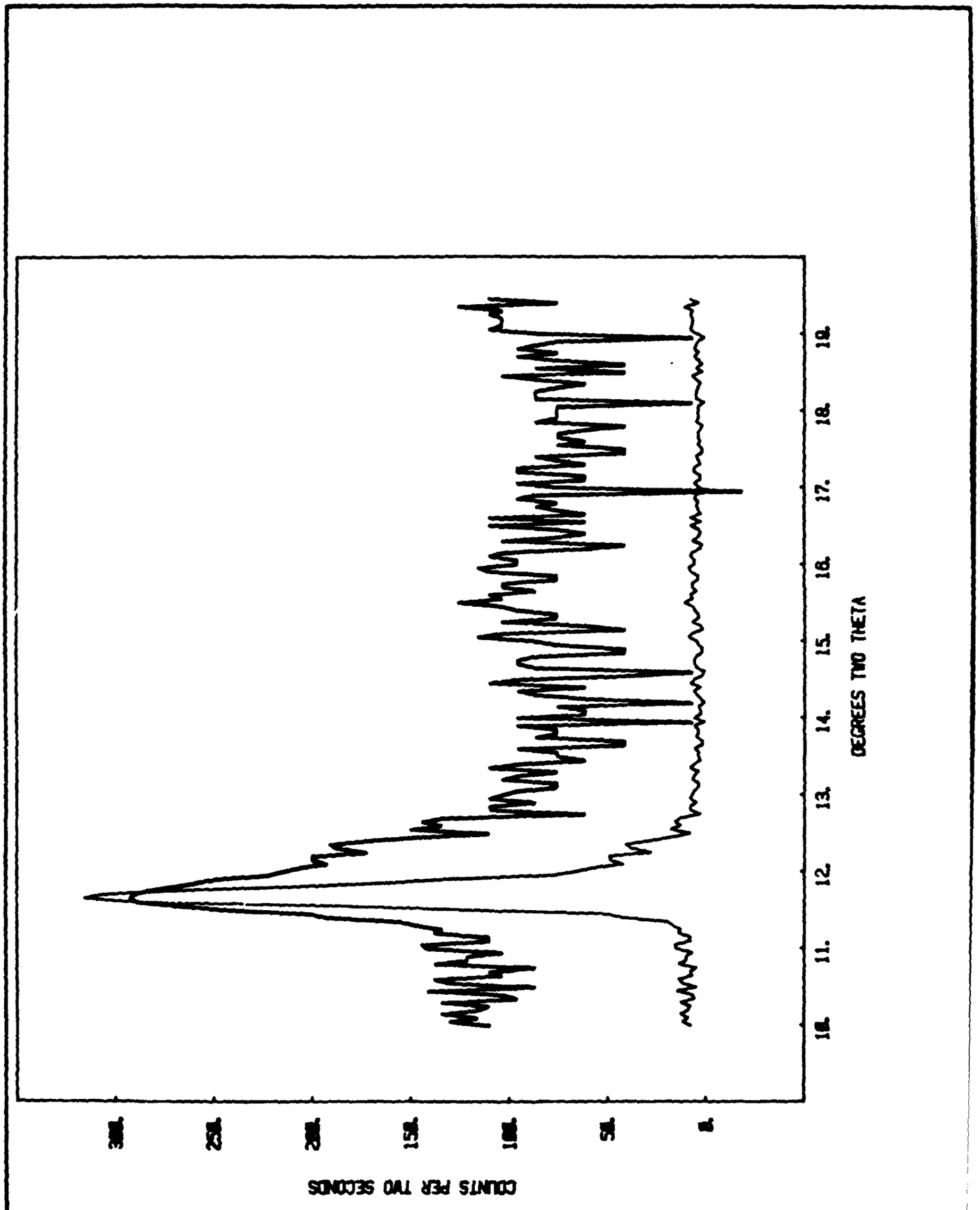
COUNTS PER TWO SECONDS
300.
250.
200.
150.
100.
50.
0.
10.
11.
12.
13.
14.
15.
16.
17.
18.
19.
DEGREES TWO THETA

Figure 7(b)

Figure 8

COUNTS PER TWO SECONDS
0
500
1000
1500
2000
6.5
7.0
7.5
8.0
8.5
DEGREES TWO THETA

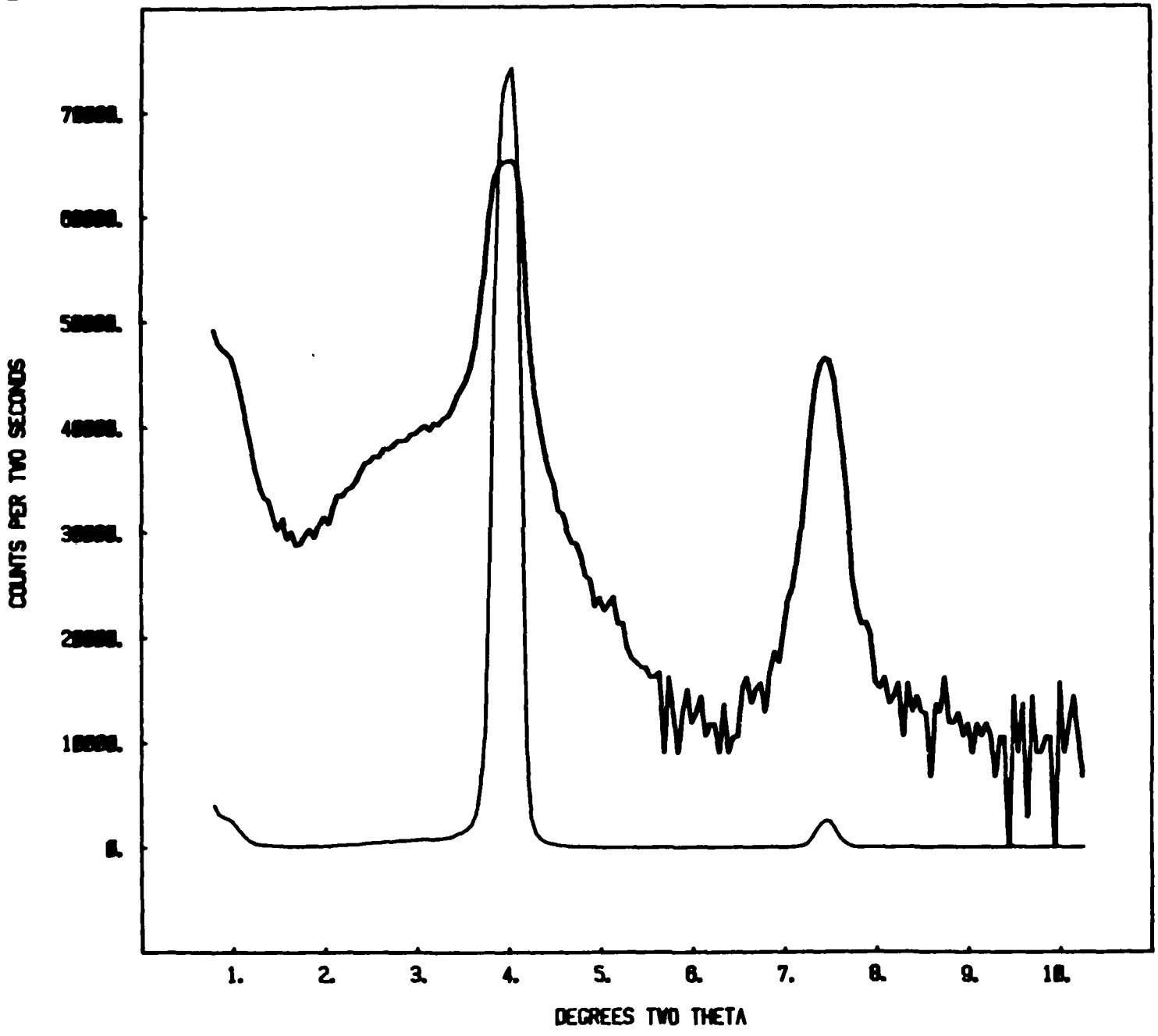

Figure 9(a)

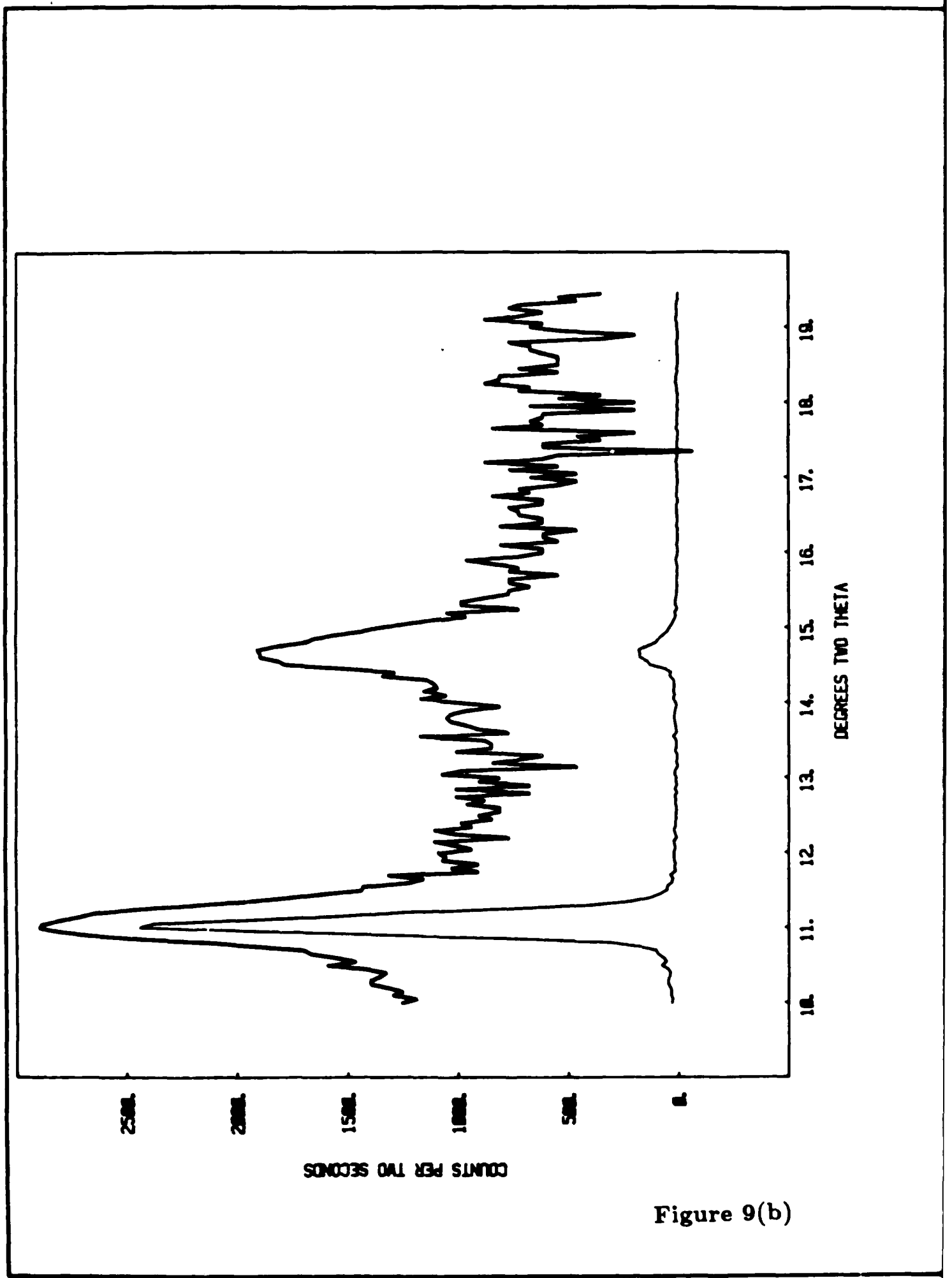
COUNTS PER TWO SECONDS
250.
200.
150.
100.
50.
0.
10.
11.
12.
13.
14.
15.
16.
17.
18.
19.
DEGREES TWO THETA

Figure 9(b)

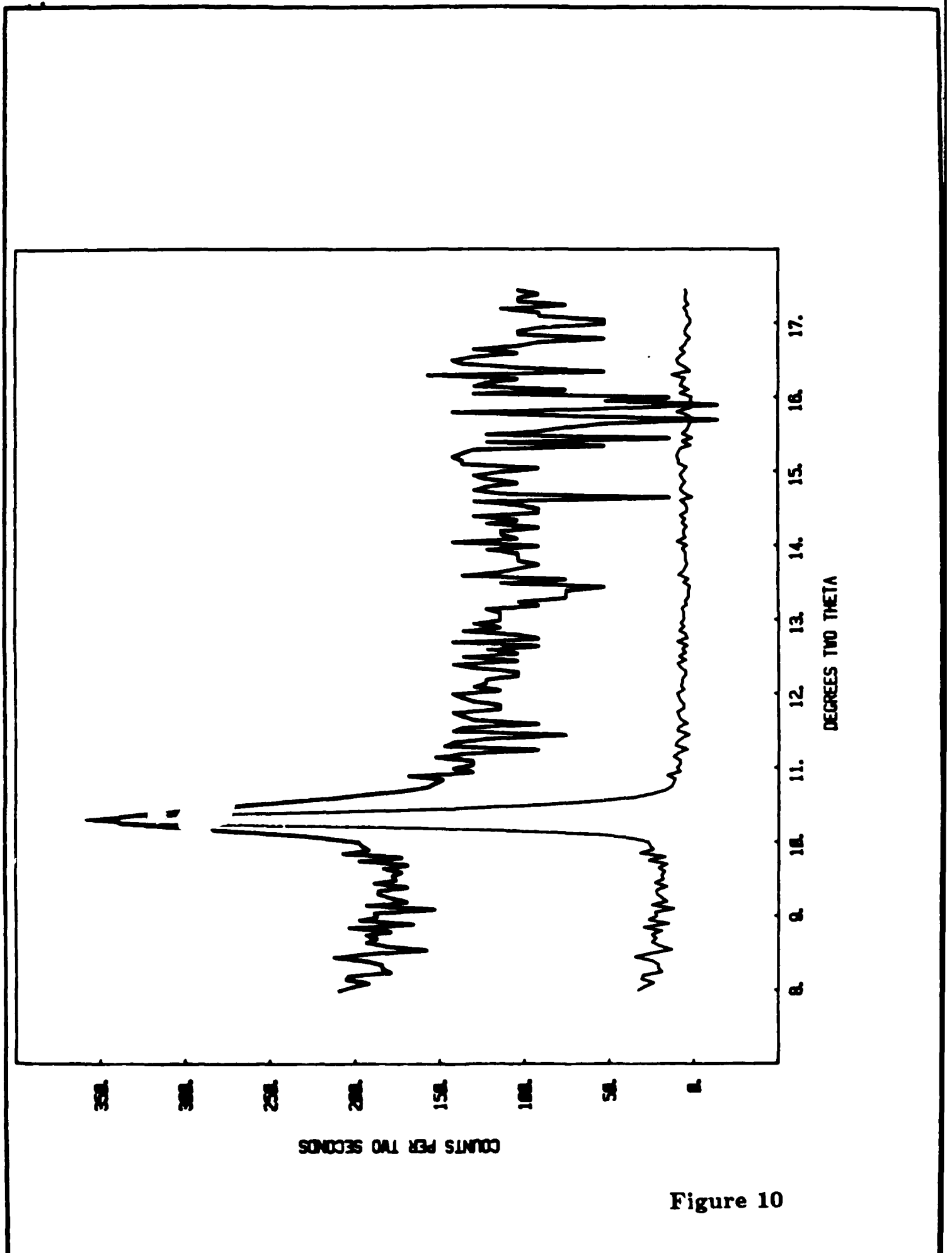
COUNTS PER TWO SECONDS
350.
300.
250.
200.
150.
100.
50.
0.
0.
1.
2.
3.
4.
5.
6.
7.
8.
9.
10.
11.
12.
13.
14.
15.
16.
17.
DEGREES TWO THETA

Figure 10

END

11-87

DTIC